Title

Atmospheric humidity regulates same-sex mating in Candida albicans through the trehalose and osmotic signaling pathways

Journal

Science China Life Sciences, 66(8)

ISSN

1674-7305

Authors

Li, Chao

Tao, Li

Guan, Guobo

et al.

Publication Date

2023-08-01

DOI

10.1007/s11427-023-2309-1

Peer reviewed

HHS Public Access

Author manuscript

Sci China Life Sci. Author manuscript; available in PMC 2023 November 08.

Published in final edited form as:

Sci China Life Sci. 2023 August ; 66(8): 1915–1929. doi:10.1007/s11427-023-2309-1.

Atmospheric humidity regulates same-sex mating in *Candida albicans* through the trehalose and osmotic signaling pathways

Chao Li[1,2,†], **Li Tao**[1,†], **Guobo Guan**[1,2,†], **Zhangyue Guan**[1], **Austin M. Perry**[3,4], **Tianren Hu**[1], **Jian Bing**[1], **Ming Xu**[1], **Clarissa J. Nobile**[3,5], **Guanghua Huang**[1,6,7,*]

[1]Department of Infectious Diseases, Huashan Hospital, Shanghai Institute of Infectious Disease and Biosecurity and State Key Laboratory of Genetic Engineering, School of Life Sciences, Fudan University, Shanghai 200438, China

[2]State Key Laboratory of Mycology, Institute of Microbiology, Chinese Academy of Sciences, Beijing 100101, China

[3]Department of Molecular and Cell Biology, University of California, Merced, Merced CA 95343, USA

[4]Quantitative and Systems Biology Graduate Program, University of California, Merced, Merced CA 95343, USA

[5]Health Sciences Research Institute, University of California, Merced, Merced CA 95343, USA

[6]Shanghai Engineering Research Center of Industrial Microorganisms, Shanghai 200438, China

[7]Shanghai Huashen Institute of Microbes and Infections, Shanghai 200052, China

Abstract

Sexual reproduction is prevalent in eukaryotic organisms and plays a critical role in the evolution of new traits and in the generation of genetic diversity. Environmental factors often have a direct impact on the occurrence and frequency of sexual reproduction in fungi. The regulatory effects of atmospheric relative humidity (RH) on sexual reproduction and pathogenesis in plant fungal pathogens and in soil fungi have been extensively investigated. However, the knowledge of how RH regulates the lifecycles of human fungal pathogens is limited. In this study, we report that low atmospheric RH promotes the development of mating projections and same-sex (homothallic) mating in the human fungal pathogen *Candida albicans*. Low RH causes water loss in *C. albicans* cells, which results in osmotic stress and the generation of intracellular reactive oxygen species (ROS) and trehalose. The water transporting aquaporin Aqy1, and the G-protein coupled receptor Gpr1 function as cell surface sensors of changes in atmospheric humidity. Perturbation of the trehalose metabolic pathway by inactivating trehalose synthase or trehalase

*Corresponding author (huanggh@fudan.edu.cn).
†Contributed equally to this work

Compliance and ethics

Clarissa J. Nobile is a cofounder of BioSynesis, Inc., a company developing diagnostics and therapeutics for biofilm infections. The other authors declare that they have no conflict of interest.

SUPPORTING INFORMATION

The supporting information is available online at https://doi.org/10.1007/s11427-023-2309-1. The supporting materials are published as submitted, without typesetting or editing. The responsibility for scientific accuracy and content remains entirely with the authors.

promotes same-sex mating in *C. albicans* by increasing osmotic or ROS stresses, respectively. Intracellular trehalose and ROS signal the Hog1-osmotic and Hsf1-Hsp90 signaling pathways to regulate the mating response. We, therefore, propose that the cell surface sensors Aqy1 and Gpr1, intracellular trehalose and ROS, and the Hog1-osmotic and Hsf1-Hsp90 signaling pathways function coordinately to regulate sexual mating in response to low atmospheric RH conditions in *C. albicans*.

Keywords

atmospheric relative humidity; sexual reproduction; same-sex mating; *Candida albicans* ; trehalose metabolism; osmotic stress

INTRODUCTION

Sexual reproduction in fungi provides genetic diversity and favorable mutations to adapt to diverse environmental niches (Barton and Charlesworth, 1998; Coelho et al., 2017; Hirakawa et al., 2017; Ni et al., 2011). Several environmental factors are known to impact the occurrence and frequency of sexual reproduction in fungi (Berman and Hadany, 2012; Guan et al., 2019; Kis-Papo et al., 2003; Ni et al., 2011; Wallen and Perlin, 2018). For example, changes in atmospheric relative humidity (RH), nutrient availability, and temperature are known to be involved in the regulation of sexual reproduction and pathogenesis in plant fungal pathogens (Clarkson et al., 2014; Granke and Hausbeck, 2010; Manstretta and Rossi, 2016; Paul and Munkvold, 2005). Despite this knowledge in plant fungal pathogens, studies on understanding how changes in environmental factors outside of the host, such as RH and climate, impact the lifecycles of human fungal pathogens are limited.

Candida species, such as *Candida albicans*, are opportunistic fungal pathogens and commensals of humans (Berman, 2012), and thus they tend to be isolated in clinical settings from human hosts. There is, however, increasing evidence to suggest that *Candida* species are also found in non-clinical natural environments, such as on trees, fruits, and in the soil (Bensasson et al., 2019; Mok et al., 1984; Nunn et al., 2007; O'Brien et al., 2021; Opulente et al., 2019). Given their persistence in and adaptation to diverse ecological niches, the lifecycles of *Candida* species are likely much more complex than our current understanding.

C. albicans is the most frequently isolated fungal species in clinical settings (Cheng et al., 2004; Guinea, 2014; Pfaller et al., 2004; Xiao et al., 2020). It is a diploid fungus that typically reproduces clonally in nature (Berman, 2012), but is also known to undergo opposite-sex (heterothallic) and same-sex (homothallic) mating under certain conditions (Alby et al., 2009; Guan et al., 2019; Miller and Johnson, 2002; Tao et al., 2014). To mate, *C. albicans* must first become homozygous (**a**/**a** or α/α) at the mating type like (*MTL*) locus or lose one allele (becoming **a**/Δ or Δ/α) at the *MTL* locus and then undergo an epigenetic phenotypic switch from the "sterile" white cell type to the mating-competent opaque cell type (Miller and Johnson, 2002). Other than mating competency, white and opaque cells of *C. albicans* also differ in cellular morphologies, virulence levels in infection models, and antifungal drug susceptibilities (Anderson and Soll, 1987; Craik et al., 2017;

Miller and Johnson, 2002; Slutsky et al., 1987). Given the tendency of *C. albicans* to clonally reproduce in nature, we previously proposed that homothallic mating could be a major mode of sexual reproduction in *C. albicans* (Guan et al., 2019). *C. albicans* often encounters nutrient limitation in its natural ecological niches, such as in the human gut. We found that glucose starvation promotes same-sex mating in *C. albicans* by increasing intracellular reactive oxygen species (ROS) and activating the Hsf1-Hsp90 stress response pathway, which in turn regulates the transcription factors Cta4 and Cwt1 (Guan et al., 2019). Cta4 interacts with Hsp90 under certain stress conditions and functions as a transcriptional repressor of *CWT1* (Diezmann et al., 2012; Guan et al., 2019; O'Meara et al., 2016). These transcription factors directly control same-sex mating in *C. albicans* by regulating the master regulator of **a**-type mating, *MTL**a**2*. Thus, the Hsf1-Hsp90 stress response pathway can regulate *C. albicans* mating under conditions of glucose starvation (Guan et al., 2019).

While generating genetic diversity through sexual reproduction is a means to survive stressful environments at a population level, individual cells must still withstand harsh environmental conditions in order to mate. In fungi such as *Saccharomyces cerevisiae* and in many plant fungal pathogens, cells accumulate trehalose, a nonreducing sugar and stress protectant, during the stationary phase and in response to conditions of nutrient depletion, low humidity, and dehydration (Eleutherio et al., 1993; Lillie and Pringle, 1980; Tapia et al., 2015). Trehalose counteracts intracellular ROS accumulation and protects protein integrity in fungi by interacting with proteins and phospholipids to maintain cell membrane structure (Estruch, 2000; Feofilova et al., 2014; Wiemken, 1990). *C. albicans* also accumulates intracellular trehalose in response to harsh environmental conditions, such as thermal and oxidative stresses (Argüelles, 2000; Estruch, 2000; Feofilova et al., 2014; Wiemken, 1990). In *C. albicans* as well as in other human fungal pathogens, the trehalose biosynthesis pathway is involved in the regulation of multiple biological processes, such as morphological transitions and pathogenesis (Serneels et al., 2012; Zaragoza et al., 1998). The accumulation of intracellular trehalose causes osmotic changes in fungal cells, activating the Hog1 osmotic sensing pathway and the Hsf1-Hsp90 stress signaling pathway (Rodaki et al., 2009; Serneels et al., 2012). This ability may represent a conserved and adaptive strategy for microorganisms to survive hostile environmental conditions.

Studies in plant fungal pathogens demonstrate that changes in atmospheric RH are a predisposing factor in the expression of virulence factors and disease epidemics (Velásquez et al., 2018). For example, in *Fusarium graminearum*, the production of perithecia and ascospores was shown to increase as RH increases (Manstretta and Rossi, 2016). In *Phytophthora capsica*, higher levels of virulence were observed as RH increases (up to 100% RH) (Granke and Hausbeck, 2010). In the rice pathogen *Magnaporthe oryzae*, RH levels were shown to have significant effects on its colonization and conidiation (Li et al., 2014). Together, these studies demonstrate that plant fungal pathogens sense and respond to fluctuations in RH, and that increased RH generally correlates with increased virulence (and/or virulence associated features).

Many superficial infections of humans caused by fungi exhibit seasonal dependencies, which are associated with changes in environmental RH (Donders et al., 2022; Khoo et al., 2020; Sharma and Nonzom, 2021). For example, talaromycosis cases caused by the

pathogen *Talaromyces marneffei* have been observed to increase by up to 30% during the rainy months (May through November) (Bulterys et al., 2013) and vaginal infections caused by certain *Candida* species have been correlated with seasonal environmental changes in some countries (Donders et al., 2022).

It has been shown that stressful conditions facilitate the parasexual cycle in *C. albicans*, including the loss of one mating type allele and induction of phenotypic switching (Alby and Bennett, 2009; Berman and Hadany, 2012; Forche et al., 2011). In this study, we found that low atmospheric RH promotes same-sex mating in *C. albicans* under conditions of glucose depletion. Low RH causes osmotic and oxidative stresses in *C. albicans* cells. We show that trehalose metabolism and the downstream Hog1-osmotic, and Hsf1-Hsp90 signaling pathways are involved in the regulation of low humidity-induced same-sex mating in this important human fungal pathogen.

RESULTS

Factors influencing mating projection formation and same-sex mating in *C. albicans*

We previously reported that depletion of glucose induces the development of mating projections and same-sex mating in *C. albicans* (Guan et al., 2019). We observed several interesting and serendipitous phenomena in this prior study that inspired the current study. First, we noticed that glucose depletion induced mating projection formation and same-sex mating under solid medium culture conditions (on nutrient YP-K plates) but not in liquid medium. Second, we observed that the mating response exhibited regional differences, such that when the same experiments were conducted under atmospheric conditions, the same-sex mating efficiencies of *C. albicans* were significantly higher when the assays were performed in Beijing, China (39°90′ N/116°40′ E) than when they were performed in Shanghai, China (31°41′ N/121°29′ E). Moreover, this phenomenon also displayed seasonal dependencies, such that the mating efficiencies were overall much higher in the less humid months in China (November through April) than in the more humid months in China (May through October). Third, *C. albicans* formed more mating projections and formed them in a relatively shorter timeframe on drier YP-K medium plates than on moister YP-K medium plates (Figure S1 in Supporting Information). Based on these preliminary observations, we hypothesized that low atmospheric RH or dehydration conditions could promote the development of mating projections and same-sex mating in *C. albicans*.

Low atmospheric RH promotes the development of mating projections in *C. albicans*

To test the hypothesis that low RH promotes the development of mating projections, we performed mating projection formation assays under 20% RH, 50% RH, and 80% RH conditions in humidity controlled cabinets. The glucose-depleted YP-K medium plates were dried for 4 days under 60% RH before use. Opaque cells were spotted onto the plates and incubated at 25°C under different RH conditions. After 3 days of incubation, approximately 3% of cells of the wildtype (WT) strain SN152**a** developed mating projections under 20% RH, while no mating projections were observed under 50% RH or 80% RH (Figure 1A). After 5 days of incubation, the percentages of projected cells were 30%±3%, 5%±2%, and <0.5% (i.e., not observed) under 20% RH, 50% RH, and 80% RH, respectively

(Figure 1A). To verify that distinct mating responses occur under the different RH conditions, we examined the relative expression levels of four mating-associated genes: *STE2*, *MFA1*, *FUS1*, and *FIG1*, encoding the α-pheromone receptor, **a**-factor precursor, and two membrane proteins required for efficient mating, respectively (Guan et al., 2019). As shown in Figure 1B, the relative expression levels of all four of the mating-associated genes under 20% RH were significantly higher than those under 50% RH and 80% RH. The relative expression levels of *FUS1* and *FIG1* under 50% RH were significantly higher than those under 80% RH. These findings indicate that low atmospheric humidity promotes the development of mating projections and the expression of mating-associated genes in *C. albicans*.

Low atmospheric RH promotes same-sex mating in *C. albicans*

A direct effect of the activation of mating-associated genes and mating projection formation is to promote sexual mating in *C. albicans* (Tao et al., 2014). We next performed quantitative mating assays and examined the effect of decreased environmental humidity on mating efficiency. As shown in the upper panel of Figure 2A, the mating mixtures of two "**a**" strains: SN250**a** and GH1013**a** cultured under 20% RH and 50% RH contained obvious projections and fusion cells, whereas no projections or fusion cells were observed in the mixture cultured under 80% RH. Consistently, mating products were observed in the 20% RH and 50% RH mixtures when the cultures were plated on selective medium, whereas no mating products were observed in the mixtures from the 80% RH plated cultures (Figure 2A, lower panel). Flow cytometry analysis demonstrated that the mating products were tetraploid cells (Figure 2B). Quantitative mating assays demonstrated that *C. albicans* underwent more efficient same-sex mating under lower RH conditions compared with higher RH conditions after 5 days of co-culture of the two mating partners (Table 1).

Low atmospheric RH leads to an increase in intracellular trehalose and ROS in *C. albicans*

Fungal cells often accumulate trehalose and ROS in response to stresses such as nutrient depletion, dehydration, and oxidative stress (Estruch, 2000). Trehalose functions as a key factor for surviving desiccation in fungi (Eleutherio et al., 1993; Serneels et al., 2012; Tapia et al., 2015; Wiemken, 1990), while the accumulation of ROS is associated with the activation of the mating response in *C. albicans* (Guan et al., 2019). We next examined the intracellular levels of trehalose and ROS under different RH conditions. As shown in Figure 3, intracellular trehalose levels were remarkably higher under 20% RH than under 50% RH and 80% RH after 5 days of incubation. At 5 days of incubation, the intracellular ROS levels exhibited an inverse relationship to atmospheric RH (Figure S2 in Supporting Information). Together, these findings indicate that low atmospheric humidity causes an increase in intracellular trehalose and ROS in *C. albicans*.

To assess the effects of increased intracellular trehalose on same-sex mating, we deleted *NTH1*, which encodes a cytoplasmic trehalase in *C. albicans*, and performed mating projection formation and quantitative mating assays. As expected, the deletion of *NTH1* led to an increase in intracellular trehalose (Figure 3) and ROS (Figure S2 in Supporting Information). The *nth1*/*nth1***a** mutant strain formed more mating projections compared with the WT strain under the 3 RH conditions after 5 days of incubation (Table 2, Figure 1A

served as the WT control). Consistently, the *nth1*/*nth1***a** mutant strain exhibited a high same-sex mating efficiency under the 3 different RH conditions (Table 1). We also found that the addition of exogenous trehalose promoted the development of mating projections and same-sex mating in *C. albicans* under the different RH conditions (Figure S3 in Supporting Information). Moreover, the addition of exogenous α-pheromone to the medium led to the increase of intracellular levels of trehalose (Figure S4A in Supporting Information) and ROS (Figure S4B in Supporting Information). Taken together, these results suggest that trehalose and its metabolism play critical roles in the regulation of low humidity-induced same-sex mating in *C. albicans*.

The aquaporin Aqy1, G-protein-coupled receptor Gpr1, and Hog1-osmotic signaling pathway regulate low humidity sensing and same-sex mating in *C. albicans*

The aquaporin Aqy1 is a water transporting protein important for responding to changes in environmental humidity in fungi (Soveral et al., 2011). To evaluate the role of Aqy1 in the regulation of low atmospheric humidity-induced mating in *C. albicans*, we deleted *AQY1* in *C. albicans* and found that compared with the WT control strain, the *aqy1*/*aqy1***a** mutant strain showed a significantly increased ability to form mating projections and to undergo same-sex mating under different RH conditions (Figure 4A and Table 1).

Gpr1 is a cell surface protein that functions as a nutrient and stress sensor and is associated with the Hog1 osmotic signaling pathway in fungi (Serneels et al., 2012). We, therefore, next examined the effects of inactivation of Gpr1 and Hog1 signaling on same-sex mating in *C. albicans*. As shown in Figure 4 and Table 1, deletion of *GPR1* and *HOG1* enhanced mating projection formation and the efficiency of same-sex mating in *C. albicans*. As expected, deletion of *PBS2* (encoding the upstream MAPK kinase of Hog1) had a similar effect in promoting the development of mating projections (Table 2). As expected, the *AQY1* and *GPR1* reconstituted strains exhibited similar abilities to undergo mating projection development compared with the WT strain. Remarkably, the *hog1*/*hog1***a** mutant strain even exhibited high levels of mating projection formation and mating efficiency under the 80% RH condition (Figure 4A and Table 1). We also found that the addition of exogenous α-pheromone to the medium increased the relative expression level of *HOG1* (Figure S4C in Supporting Information). Quantitative real-time PCR (qRT-PCR) assays indicated that the expression of *GPR1* was induced under the 20% RH condition (Figure 4B). Consistently, deletion of *GPR1* resulted in a reduced level of Hog1 phosphorylation, especially under high humidity conditions (Figure 4C), suggesting that Gpr1 functions upstream of the Hog1 signaling pathway. Moreover, deletion of *GPR1* led to decreases in the levels of intracellular trehalase (Figure S5A in Supporting Information) and decreases in the relative expression levels of *AQY1* under different humidity conditions (Figure S5B in Supporting Information), implying that Aqy1 may function through Gpr1 and the Hog1 signaling pathway in the regulation of humidity sensing and same-sex mating in *C. albicans*. Consistently, we found that deletion of *AQY1*, *GPR1*, or *HOG1* had similar effects on increasing intracellular trehalose and ROS levels (Figure 3; Figure S2 in Supporting Information). This accumulation of intracellular trehalose could cause osmotic stress and lead to the activation of the mating response.

Role of the trehalose synthesis pathway in same-sex mating in *C. albicans*

Trehalose protects protein integrity in fungi under conditions of oxidative stress (Argüelles, 2000). As shown above, the increased intracellular levels of both trehalose and ROS affect mating in *C. albicans*. We next examined the role of the trehalose-6-phosphate synthase Tps1 and the trehalose-6-phosphate phosphatase Tps2 in the regulation of same-sex mating in *C. albicans*. As shown in Figure 3, deletion of *TPS1* but not *TPS2* led to decreased levels of intracellular trehalose. Consistently, deletion of *TPS1* led to increased levels of intracellular ROS (Figure S2 in Supporting Information). The *tps1*/*tps1***a** but not *tps2*/*tps2***a** mutant strain exhibited an increased ability of mating projection formation and same-sex mating under different RH conditions (Tables 1 and 2). Consistently, overexpression of the trehalase-encoding gene *NTH1* resulted in decreased levels of intracellular trehalose and increased levels of ROS and thus had a promoting effect on mating projection formation and same-sex mating in *C. albicans* (Figure S6 in Supporting Information).

Previous studies indicate that the glyoxylate shunt is involved in the regulation of trehalose biosynthesis and low humidity tolerance in both *Caenorhabditis elegans* and *S. cerevisiae* (Erkut et al., 2016). As shown in Figure 3, deletion of *ICL1* (encoding an isocitrate lyase) or *MLS1* (encoding a malate synthase) in *C. albicans* led to lowered intracellular levels of trehalose compared with the WT strain. Similar to the *tps1*/*tps1***a** mutant strain, the *icl1*/*icl1***a** and *mls1*/*mls1***a** mutant strains exhibited higher abilities of mating projection formation and same-sex mating under different RH conditions compared with the WT strain (Tables 1 and 2). qRT-PCR assays demonstrated that deletion of *AQY1* resulted in increased expression of *TPS1*, *ICL1*, and *MLS1*, indicating a negative role of Aqy1 in the regulation of the glyoxylate shunt and in trehalose biosynthesis (Figure S5C in Supporting Information). These findings are consistent with the finding that deletion of *AQY1* led to an increase of intracellular trehalose.

Given the protective effects of trehalose on oxidative stress in *C. albicans*, we next determined the ROS levels in the *tps1*/*tps1***a**, *icl1*/*icl1***a**, and *mls1*/*mls1***a** mutant strains. As shown in Figure S2 in Supporting Information, the intracellular ROS levels in these mutant strains were increased under all 3 RH conditions compared with the WT strain. Taken together, these results indicate that disruption of trehalose synthesis leads to decreases in intracellular trehalose and the accumulation of intracellular ROS that promote same-sex mating in *C. albicans*.

As aforementioned, multiple signal pathways are involved in the regulation of trehalose metabolism and the inactivation of trehalose synthesis-associated genes not only cause the reduced intracellular level of trehalose but also the elevated level of intracellular ROS. We next deleted *CAP1*, encoding bZIP transcription factor involved in stress response, in the *C. albicans* WT strain. Compared with the WT strain, the increase of the intracellular ROS level of the *cap1*/*cap1* mutant was limited under low humidity conditions (Figure S2 in Supporting Information). However, the intracellular trehalose level of the *cap1*/*cap1* mutant was significantly decreased (Figure 3). As expected, the inactivation of *CAP1* resulted in a remarkable reduced ability of the development of mating projections (Table 2) and same-sex

mating (Table 1). These findings further verified the close association between trehalose metabolism and low humidity-induced same-sex mating in *C. albicans*.

Role of the Hsf1-Hsp90 signaling pathway in same-sex mating in *C. albicans*

Since the Hsf1-Hsp90 signaling pathway plays critical roles in the response of *C. albicans* to oxidative and osmotic stresses (Guan et al., 2019; Serneels et al., 2012), we next examined the mating projection formation abilities of conditional mutants of *HSF1* and *HSP90* under different RH conditions. As shown in Table 2, both the *tetON-HSF1*/*hsf1* and *tetON-HSP90*/*hsp90* mutant strains were able to undergo robust mating projection formation under 20% RH, 50% RH, and 80% RH, suggesting that downregulation of the Hsf1-Hsp90 signaling pathway overrides the repressing effects of high environmental humidity on the mating response. Of note, doxycycline, which induces the Tet-On promoter system, only slightly affected these processes possibly due to the "leaky" expression of TETp-*HSP90* and TETp-*HSF1* in opaque cells.

Cwt1 and Cta4 are transcription factors downstream of the Hsf1-Hsp90 signaling pathway that play opposing roles in the regulation of glucose depletion-induced same-sex mating in *C. albicans* (Guan et al., 2019). As expected, the *cwt1*/*cwt1***a** mutant strain showed an enhanced ability to form mating projections under 20% RH, 50% RH, and 80% RH, while the *cta4*/*cta4***a** mutant strain was incapable of forming mating projections even under 20% RH (Table 2). These results suggest that the Hsf1-Hsp90 signaling pathway plays an important role in the regulation of low humidity-induced same-sex mating in *C. albicans*. The osmotic stresses resulting from lowered trehalose levels and the oxidative stresses resulting from increased ROS could converge on the Hsf1-Hsp90 pathway to activate the mating response in *C. albicans* under conditions of low environmental humidity.

DISCUSSION

Atmospheric humidity is an important environmental factor affecting the pathogenesis and sexual reproduction of plant fungal pathogens (Clarkson et al., 2014; Granke and Hausbeck, 2010; Li et al., 2014; Paul and Munkvold, 2005). Some fungi depend on their sexual cycles to survive over dry and cold seasons (Hassine et al., 2019; Wallen et al., 2021). Recent studies demonstrate that seasonality and more importantly environmental RH influence the prevalence and severity of superficial infections caused by human fungal pathogens (Donders et al., 2022; Sharma and Nonzom, 2021). In addition, adverse environmental conditions often suppress vegetative cell growth and promote sexual reproduction in fungi (Berman and Hadany, 2012; Guan et al., 2019; Ni et al., 2011). This inverse relationship observed between vegetative (i.e., non-sexual) growth and sexual reproduction under certain environmental conditions could be due to the increased vulnerability of vegetatively grown cells compared with sexual spores in harsh environments. In addition, compared with vegetative growth, sexual reproduction produces more genetically diverse offspring that can adapt to different environmental niches. As a common commensal fungus of humans that often resides on the skin, it would make sense that *C. albicans* experiences and adapts to changing RH conditions during different environmental seasons and that these fluctuating conditions should affect the lifecycle of *C. albicans*. Moreover, *C. albicans* and

its closely related species have been isolated in non-clinical settings, such as in soil and on plants (Bensasson et al., 2019; Opulente et al., 2019), indicating that *C. albicans* persists in the external environment and readily experiences changing RH conditions. Here we provide evidence demonstrating that environmental RH regulates the development of mating projections and same-sex mating in *C. albicans*, suggesting that humidity plays an important role in the regulation of sexual reproduction in this prevalent human pathogen.

In the current study, we show that environmental humidity functions as a critical regulator of same-sex mating in *C. albicans* under low humidity conditions. As presented in the regulatory model in Figure 5, the G-protein coupled receptor Gpr1 and the water transporting aquaporin Aqy1 function as cell surface sensors of atmospheric humidity. The low humidity stress signal then activates the synthesis of trehalose and the generation of ROS in *C. albicans* cells. Moreover, glucose depletion may have an additive effect on the generation of intracellular ROS due to active oxidative metabolism. In response to the accumulation of ROS, the Hsf1-Hsp90 signaling pathway is activated and becomes overwhelmed. Meanwhile, the accumulation of intracellular trehalose increases intracellular osmotic stress on the cells and signals the Hog1 signaling pathway, which subsequently converges on the Hsf1-Hsp90 signaling pathway. Therefore, the cell surface sensors, intracellular trehalose, intracellular ROS, and the Hog1 and Hsf1-Hsp90 signaling pathways may function coordinately to regulate low atmospheric humidity-induced same-sex mating in *C. albicans*.

Given that low environmental RH leads to water loss in *C. albicans* cells, it is likely that the water transporting aquaporin Aqy1 and the Hog1-osmotic signaling pathway are involved in the regulation of this process (Figure 5). Under conditions of low environmental RH, we show that trehalose accumulates in *C. albicans* cells (Figure 3), which has multiple functions including protecting the cell membrane and stabilizing proteins upon nutrient, oxidative, dehydration, and osmotic stresses (Elbein et al., 2003; Feofilova et al., 2014). Interestingly, we found that inactivation of either the trehalose degradation- or biosynthesis-associated genes (e.g., *NTH1* and *TPS1*) had similar effects on the induction of same-sex mating in *C. albicans* (Figure 3 and Table 1). One possible explanation for this finding is that intracellular trehalose and ROS coordinately control various downstream pathways. Deletion of *NTH1* leads to an accumulation of intracellular trehalose and an increase in osmotic stress on the cell, which activates the Hog1-osmotic signaling pathway; whereas inactivation of *TPS1*, *ICL1*, or *MLS1* results in a decrease in intracellular trehalose and an increase in ROS (Figure 3; Figure S2 in Supporting Information).

The Hog1 signaling pathway plays a critical role in stress response in *C. albicans* (Enjalbert et al., 2006). Here we showed that deletion of *HOG1* resulted in trehalose accumulation and increased same-sex mating in *C. albicans* (Figure 3 and Table 1), suggesting an association between trehalose, osmotic stress, and the Hog1 signaling pathway. The persistence of trehalose at high concentrations inhibits chaperone-mediated protein refolding (Jain and Roy, 2009). Therefore, trehalose must be rapidly degraded by trehalase (Nth1) to allow for the reactivation of denatured proteins by molecular chaperones under stressful conditions (Singer and Lindquist, 1998). Our results show that low humidity or Gpr1 dysfunction leads to a decreased activity of Nth1 and persistent accumulation of trehalose (Figure 3;

Figure S5 in Supporting Information), which could have an inhibitory effect on the function of chaperones, such as Hsp90 and Hsp104. Trehalose, therefore, may coordinate with the Hsp90 pathway in the control of protein integrity (Singer and Lindquist, 1998).

Glucose-depleted YP-K medium was used in our study for all mating responses and quantitative mating assays. Glucose depletion may have an additive effect on intracellular ROS accumulation. As shown in Figure S2 in Supporting Information, the mutant strains with the strongest responses to low humidity-induced mating displayed increased intracellular ROS levels, implying that ROS plays a central role in this regulation. The Hog1-osmotic and ROS signaling pathways converge on the Hsf1-Hsp90 pathway to regulate the mating response in *C. albicans* via the transcription factors Cta4, Cwt1, and MTLa2 (Guan et al., 2019) (Figure 5).

C. albicans can undergo both opposite-sex (heterothallic) and same-sex (homothallic) mating under certain conditions (Alby et al., 2009; Guan et al., 2019; Tao et al., 2014). A prerequisite for opposite-sex mating is the physical proximity of opposite *MTL* mating partners ("**a**" and "α"). Given the clonal growth nature of *C. albicans*, the chances of such mating events to occur are improbable. Unlike *S. cerevisiae* and *Schizosaccharomyces pombe*, *C. albicans* lacks the homothallic switching (HO) endonuclease and is unable to undergo mating type switching. Previous studies demonstrated that inactivation of the Bar1 protease or the Yci1 domain protein Ofr1 confers the ability of same-sex mating in *C. albicans* (Sun et al., 2016). Natural mutations in *BAR1* or *OFR1*, however, have not been observed in clinical isolates of *C. albicans*. Low environmental humidity and glucose depletion stresses, on the other hand, are frequently encountered by *C. albicans* in its natural ecological niches. Therefore, same-sex mating induced by these conditions may represent a common sexual reproduction strategy in this fungal pathogen.

CONCLUSIONS

Relative atmospheric humidity has a plethora of effects on the lifecycles of fungi. Here we report that low humidity promotes same-sex mating in the human fungal pathogen *C. albicans*, highlighting the conserved feature of humidity sensing in fungi. Trehalose metabolism and ROS play central roles in this regulation via the Hog1-osmotic and Hsf1-Hsp90 stress response signaling pathways. The promoting effect of low humidity on sexual reproduction could benefit the fungus by generating genetic and phenotypic diversity to adapt to environmental changes. Our findings provide new evidence showing that *C. albicans* adopts multiple strategies to undergo sexual reproduction under stressful conditions and provide a mechanism by which sexual reproduction could occur frequently in nature.

MATERIALS AND METHODS

Media and culture conditions

YPD medium (20 g L^{-1} glucose, 20 g L^{-1} peptone, 10 g L^{-1} yeast extract, and 20 g L^{-1} agar) plates were used for the routine culture of *C. albicans*. Lee's GlcNAc and Lee's glucose plates were used for the induction and routine culture of opaque cells, respectively (Tao et al., 2014). Solid YP-K medium (20 g L^{-1} peptone, 10 g L^{-1} yeast extract, and 20 g

L^{-1} agar) was used for the evaluation of colony and cellular morphologies and quantitative mating assays. If not specifically stated in the text as otherwise, YP-K plates were dried at 25°C for 4 days before being used for cell growth assays. Solid synthetic complete (SCD) medium plates lacking one or two nutrients (uridine, histidine, or arginine) were used for selectable growth in quantitative mating assays.

Construction of *C. albicans* strains

Detailed information on the strains used in this study is presented in Table S1 in Supporting Information. All strains were derivatives of SN152**a** (**a**/−, *his1Δ/Δ leu2Δ/Δ arg4Δ/Δ*), SN250**a** (**a**/−, *arg4Δ/Δ*) (Noble and Johnson, 2005) or GH1013**a**h (**a**/−, *his1Δ/Δ*) (Huang et al., 2009). For convenience, *MTL***a** (or "**a**'') and *MTL*α (or "α'') presented in Figures or Tables indicate that the *MTL* loci are **a**/**a** (or **a**/Δ) and α/α (or "Δ/α''), respectively.

The fusion PCR recombination method and target gene knockout strategy (Noble and Johnson, 2005) were used to delete *TPS1*, *TPS2*, *NTH1*, *AQY1*, *GPR1*, *ICL1*, *MLS1*, *PBS2*, and *HOG1* in *C. albicans*. Primer pairs (Maker-FWD/Maker-REV) were used to amplify the selection marker expression cassettes, such as *CdHIS1*, *CmLEU2*, and *CaARG4*, from plasmids pSN52, pSN40, and pSN69 by PCR. To delete the first allele of each gene, SN152**a** was transformed with the fusion PCR products of the *CdHIS1* flanked by 5′- and 3′-flanking fragments of the target gene. To delete the second allele of the target gene, the heterozygous mutants were transformed with fusion PCR products of the *CdLEU2* or *CaARG4* flanked by 5′- and 3′-flanking fragments of the target gene. SCD amino acid dropout plates were used for prototrophic selection growth. All primers used for PCR are listed in Table S2 in Supporting Information.

Construction of plasmids

To construct the *NTH1*-overexpression plasmid pACT1-NTH1, the *NTH1* ORF cassette was amplified by PCR using primers NTH1-OE-FWD/NTH1-OE-REV (carrying *EcoR*V and *Cla*I restriction sites, respectively) from SC5314 genomic DNA and subcloned into the *EcoR*V/*Cla*I site of plasmid pACT1 (Huang et al., 2006). *Asc*I-linearized plasmids pACT1-NTH1 and pACT1 were used for the *C. albicans* transformations.

To construct the *AQY1* complementation plasmid AQY1p-AQY1, *GPR1* complementation plasmid GPR1p-GPR1, and *HOG1* complementation plasmid HOG1p-HOG1, the *AQY1*, *GPR1*, and *HOG1* 5′-fragments, respectively, were amplified by PCR using primer pairs AQY1/GPR1/HOG1 5′-fragment-FWD/REV (carrying *Apa*I and *Xho*I restriction sites, respectively) from *C. albicans* genomic DNA and subcloned into the *Apa*I/*Xho*I sites of plasmid pSFS2A (Reuß et al., 2004). Then, the *AQY1*, *GPR1*, and *HOG1* 3′-fragments were amplified by PCR using primer pairs AQY1/GPR1/HOG1 3′-fragment-FWD/REV (carrying *Sac*II and *Sac*I restriction sites, respectively) from *C. albicans* genomic DNA and subcloned into the *Sac*II/*Sac*I sites of plasmids pSFS2A-AQY1 5′, pSFS2A-GPR1 5′, and pSFS2A-HOG1 5′, respectively, generating the complementation plasmids of interest. *Apa*I/*Sac*I-linearized complementation plasmids AQY1p-AQY1, GPR1p-GPR1, and HOG1p-HOG1 were used for *C. albicans* transformation to generate the *AQY1*/*GPR1*/*HOG1* reconstituted strains, respectively. A similar strategy was used to construct the *NTH1*-complementation

plasmid NTH1p-NTH1 and the *TPS1* complementation plasmid TPS1p-TPS1. The *NTH1* 5′- and 3′-fragments were subcloned into the *Kpn*I/*Xho*I and *Sac*II/*Sac*I sites of plasmid pSFS2A, respectively. The *TPS1* 5′- and 3'-fragments were subcloned into the *Apa*I/*Sal*I and *Sac*II/*Sac*I sites of plasmid pSFS2A, respectively. All primers used are listed in Table S2 in Supporting Information.

Induction of mating projection formation in *C. albicans*

To induce the opaque phenotype, *C. albicans* cells were plated on Lee's GlcNAc medium plates and grown at 25°C for 4 days. Opaque cells collected from homogenous colonies were then replated on Lee's glucose medium plates and grown at 25°C for 5 days. Approximately 1×10^7 opaque cells in 5 μL ddH_2O of each strain from Lee's glucose medium plates were spotted onto YP-K plates and incubated under different RH levels (~20%, ~50%, and ~80%) at 25°C. Three biological repeats were performed for each strain. Of note, due to technical reasons, the 3 RH conditions (~20%, ~50%, and ~80%) fluctuated between a range of 15%–20%, 45%–50%, and 75%–80%, respectively.

Morphological analysis assays

Colony morphologies of opaque cells under different RH conditions were photographed using a stereoscopic microscope camera system (NSZ-810+Dig1600, Ningbo Yongxin Optics Co., Ltd., Ningbo, China) after 3 or 5 days of culture at 25°C. Cellular morphologies were photographed using a Leica DM2500 optical microscope (Leica Microsystems Inc., USA).

Projected opaque cell assays

To count projected opaque cells, 3 independent microscopic images/views for each strain containing approximately 300 opaque cells were selected for examination. The percentages of projected opaque cells were counted for each image and averaged.

Quantitative mating assays

Approximately 1×10^7 opaque cells (for each strain) of the two mating partners were mixed in 10 μL ddH_2O, spotted onto YP-K medium plates, and cultured at 25°C under different RH conditions for 3 or 5 days. Mating mixtures were collected in 100 μL ddH_2O and replated onto SCD-His-Leu, SCD-His, and SCD-Leu (or SCD-His-Arg, SCD-His, and SCD-Arg) dropout medium plates for prototrophic selection. After cultivation at 37°C for 2 days, the numbers of colonies on SCD amino acid-dropout plates were recorded and the mating efficiencies were calculated according to our previous publication (Tao et al., 2014).

Pheromone treatment assays

Approximately 1×10^7 opaque cells in 5 μL ddH_2O of strain SN250 were spotted onto YP-K medium plates and cultured at 25°C. 10 μL of 200 μmol L^{-1} α-pheromone (GFRLTNFGYFEPG, Beijing SciLight Biotechnology Ltd. Co., Beijing, China) was added onto the colony every day from the second day. Fungal cells were collected for RNA extraction, intracellular reactive oxygen species, and intracellular trehalose determination after 5 days.

Flow cytometry analysis

For each mating cross, approximately 10–30 colonies of mating products were collected and subject to cellular morphology and fluorescence activating cell (FACS) examination. *C. albicans* cells were initially cultured in liquid SCD amino acid-dropout medium at 30°C at 220 r min^{-1} for overnight growth. Approximately 3×10^6 cells were reinoculated into 3 mL fresh SCD medium and incubated at 30°C at 220 r min^{-1} for 3–4 h. Approximately 1×10^7 cells were collected and washed with 1×TE buffer (10 mmol L^{-1} Tris, 1 mmol L^{-1} EDTA, pH 8.0). The samples were resuspended in 0.3 mL 1×TE buffer and fixed with 0.7 mL absolute ethyl alcohol for 2 h at room temperature. The samples were washed once with 1 mL 1×TE and resuspended in 0.5 mL 1×TE before treatment with 3 mg mL^{-1} RNase A (Thermo Fisher Scientific Inc., USA) at 37°C overnight and 15 mg mL^{-1} proteinase K (Thermo Fisher Scientific Inc.) at 50°C for 2 h. After enzymolysis, the samples were washed twice with 1×TE, resuspended in 0.5 mL 1×TE, and treated with 5 μL 5 mg mL^{-1} propidium iodide (Sigma-Aldrich, USA). A total of 100,000 cells for each sample were used for flow cytometry assays. The results were analyzed using FlowJo V10 0.7 software.

Protein extraction and immunoblot assays

C. albicans cells grown under different RH conditions were harvested, washed twice with 1×PBS, and resuspended in 100 μL lysis buffer (50 mmol L^{-1} Tris-HCl/pH 8.0, 150 mmol L^{-1} NaCl, 1% NP-40, 1% Na-deoxycholate, 0.1% (w/w) SDS, 1 mmol L^{-1} EGTA, 1 mmol L^{-1} EDTA, and 1 mmol L^{-1} PMSF) containing the protease inhibitor mix (Roche Diagnostics, Germany). Cells were then subjected to 8 rounds of bead beating (50 s beating followed by 1 min cooling on ice for each round) using a Mini-BeadBeater-16 instrument (Bio Spec Products Inc., USA). The supernatant of the cell lysate was harvested by centrifugation at 4°C (14,500×*g* for 10 min), and the protein concentration was determined by Bradford protein assays (Sigma-Aldrich). An equal amount of protein in each sample was separated using SDS-PAGE (sodium dodecyl sulfate-polyacrylamide) gel assays, and then transferred to a polyvinylidene difluoride (PVDF) membrane (Millipore, USA) for Western blot detection. Hog1 phosphorylated levels were examined using a polyclonal anti-phospho p38 T180/Y182 antibody (1:1,000 dilution, Cell Signaling Technology Inc., USA). Total Hog1 protein was assessed using horseradish peroxidase (HRP)-conjugated monoclonal anti-TAP antibody (1:1,000 dilution, Sigma-Aldrich). The levels of Cdc28 protein were determined using a monoclonal anti-Cdc28 antibody (1:1,000 dilution, Santa Cruz Biotechnology Inc., USA) and served as the loading control.

RNA extraction and qRT-PCR assays

Opaque cells of *C. albicans* were grown on YP-K medium plates at 25°C for 5 days under different RH conditions and collected for total RNA extraction using the GeneJET RNA Purification Kit (Thermo Fisher Scientific Inc.). 1 μg of total RNA was used to synthesize cDNA with RevertAid H Minus First Strand cDNA Synthesis Kit (Thermo Fisher Scientific Inc.). Quantification of cDNA was performed with a Bio-Rad CFX Connect Real-time PCR Detection System (Bio-Rad, USA) using an SYBR green mix (Toyobo Co., Ltd, Japan). The fluorescence signal was detected and normalized to the expression level of *C. albicans*

ACT1. Data were analyzed using the Bio-Rad CFX Manager 3.1 software (Bio-Rad). Three biological replicates were performed for each sample.

Intracellular ROS and trehalose determination

Intracellular ROS determination assays were performed as previously reported with slight modifications (Guan et al., 2019). Approximately 1×10^5 opaque cells of *C. albicans* cultured under different RH conditions were collected for intracellular ROS determination. Fungal cells were washed with 1 mL prechilled 1×PBS and resuspended in 1 mL ddH_2O. The samples were immediately incubated with 1 μL DCFH-DA (Beyotime Biotechnology, Shanghai, China) at 37°C for 40 min. After being washed with 1×PBS twice, the samples were resuspended in 1 mL ddH_2O. The fluorescence intensity of DCF, reflecting the relative ROS level, was then rapidly measured at the excitation wavelength of 488 nm and emission wavelength of 525 nm by ELISA using the Cytation 3 plate reader (BioTek Instruments Inc., USA). Three biological replicates were performed, and the results were normalized to the cell number.

Intracellular trehalose determination assays were performed according to a previous report with slight modifications (Schulze et al., 1995). Approximately 5×10^7 opaque cells of *C. albicans* cultured under different RH conditions were collected in a 2 mL tube. Samples were washed twice with 1 mL prechilled 1×PBS and resuspended in 0.25 mL of 0.2 mol L^{-1} sodium carbonate. *C. albicans* cells were boiled at 97°C–98°C for 4 h. Then, 0.15 mL of 1 mol L^{-1} acetic acid and 0.6 mL of 0.2 mol L^{-1} sodium acetate were added to each sample. To convert intracellular trehalose to glucose, the samples were incubated with 12.5 μL trehalase (Sigma-Aldrich) at 37°C for 24 h.

To determine the glucose level in the preprocessed samples, the Glucose (GO) Assay Kit (Sigma-Aldrich) was used according to the manufacturer's instructions. After the stop reaction and chromogenic reaction, GO assays were performed using a 96-well flat-bottom microplate by adding 200 μL of the reaction products to each well. The final reaction product was monitored at the 540 nm wavelength by ELISA. The content of intracellular trehalose (mg/10^7 cells) was normalized to the glucose standard and the number of cells as follows: Glucose=(ΔA540 of Sample)×(Glucose Standard, 0.5 mg)/ΔA540 of Glucose Standard×(2×5).

Determination of the specific activity of intracellular trehalase

The samples containing 100 mg cells were collected from YP-K medium plates incubated under different RH conditions. Fungal cells were quickly washed with 1.5 mL prechilled ddH_2O and centrifuged in a 2 mL tube at 14,500×*g* for 1 min at 4°C. The samples were resuspended into 0.5 mL prechilled 50 mmol L^{-1} MES/NaOH buffer (pH 7.0) containing 50 μmol L^{-1} $CaCl_2$.

To obtain the crude enzyme extract, the samples were treated for 4–6 rounds by a Mini-BeadBeater-16 instrument for 40 s and placed on ice for 1 min between intervals. The crude enzyme extract was centrifuged at 14,500×*g* for 6 min at 4°C. 0.45 mL of the supernatant was dialyzed using a 50 kD dialysis membrane (Sangon Biotech Co., Ltd., Shanghai, China) with 5 mmol L^{-1} MES/NaOH buffer (pH 7) containing 50 pmol L^{-1} $CaCl_2$ for 12 h at 4°C.

To assess the intracellular trehalase, 10 μL crude enzyme extract from the dialysis membrane was mixed with 90 μL ddH_2O and 200 μL substrate solution (0.5 mol L^{-1} trehalose in 62.5 mmol L^{-1} MES/NaOH buffer with 125 μmol L^{-1} $CaCl_2$, pH 7), and incubated at 30°C for 30 min. The mixture was boiled to stop the hydrolysis reaction. The liberated glucose in the mixture was assayed using the GO Assay Kit. The protein (20 μL crude enzyme extract+200 μL Coomassie brilliant blue G250) was determined at the 595 nm wavelength by ELISA. Three biological repeats were performed. The final specific activity of intracellular trehalase is expressed as the rate (nmol min^{-1} mg^{-1}) of liberated glucose per unit mass and unit time as follows: Specific activity= Liberated glucose in the mixture (nmol)/Time (30 min)× Protein of 10 μL dialyzed extract (mg).

Statistical analyses

All statistical analyses in this study were performed using GraphPad Prism 8 software. qRT-PCR data were analyzed using paired Student's *t*-tests. The data of intracellular trehalose content, intracellular ROS, and specific activity of intracellular trehalase were analyzed using Q-plots and Shapiro-Wilk tests. A two-way analysis of variance (two-way ANOVA) was then performed and followed by Tukey's multiple comparison difference test. All statistical analyses were performed with a 95% confidence interval (α=0.05).

Supplementary Material

Refer to Web version on PubMed Central for supplementary material.

Acknowledgements

This work was supported by the National Key Research and Development Program of China (2021YFC2300400), the National Natural Science Foundation of China (31930005 and 32170194), and Shanghai Municipal Science and Technology Major Project (HS2021SHZX001). This work was also supported by the National Institutes of Health (NIH) National Institute of General Medical Sciences (NIGMS) award R35GM124594, and by the Kamangar family in the form of an endowed chair to C.J.N. The content is the sole responsibility of the authors and does not represent the views of the funders. The funders had no role in the design of the study; in the collection, analyses, or interpretation of data; in the writing of the manuscript; or in the decision to publish the results. We thank all members of the Huang and Nobile labs for feedback on the manuscript.

References

Alby K, and Bennett RJ (2009). Stress-induced phenotypic switching in *Candida albicans*. Mol Biol Cell 20, 3178–3191. [PubMed: 19458191]

Alby K, Schaefer D, and Bennett RJ (2009). Homothallic and heterothallic mating in the opportunistic pathogen *Candida albicans*. Nature 460, 890–893. [PubMed: 19675652]

Anderson JM, and Soll DR (1987). Unique phenotype of opaque cells in the white-opaque transition of *Candida albicans*. J Bacteriol 169, 5579–5588. [PubMed: 3316187]

Argüelles JC (2000). Physiological roles of trehalose in bacteria and yeasts: a comparative analysis. Arch Microbiol 174, 217–224. [PubMed: 11081789]

Barton NH, and Charlesworth B (1998). Why sex and recombination? Science 281, 1986–1990. [PubMed: 9748151]

Bensasson D, Dicks J, Ludwig JM, Bond CJ, Elliston A, Roberts IN, and James SA (2019). Diverse lineages of *Candida albicans* live on old oaks. Genetics 211, 277–288. [PubMed: 30463870]

Berman J (2012). Candida albicans. Curr Biol 22, R620–R622. [PubMed: 22917504]

Berman J, and Hadany L (2012). Does stress induce (para)sex? Implications for *Candida albicans* evolution. Trends Genet 28, 197–203. [PubMed: 22364928]

Bulterys PL, Le T, Quang VM, Nelson KE, and Lloyd-Smith JO (2013). Environmental predictors and incubation period of AIDS-associated *Penicillium marneffei* infection in Ho Chi Minh City, Vietnam. Clin Infect Dis 56, 1273–1279. [PubMed: 23386634]

Cheng MF, Yu KW, Tang RB, Fan YH, Yang YL, Hsieh KS, Ho M, and Lo HJ (2004). Distribution and antifungal susceptibility of *Candida* species causing candidemia from 1996 to 1999. Diag Microbiol Infect Dis 48, 33–37.

Clarkson JP, Fawcett L, Anthony SG, and Young C (2014). A model for *Sclerotinia sclerotiorum* infection and disease development in lettuce, based on the effects of temperature, relative humidity and ascospore density. PLoS ONE 9, e94049. [PubMed: 24736409]

Coelho MA, Bakkeren G, Sun S, Hood ME, and Giraud T (2017). Fungal sex: the basidiomycota. Microbiol Spectr 5, FUNK-0046–2016

Craik VB, Johnson AD, and Lohse MB (2017). Sensitivity of white and opaque *Candida albicans* cells to antifungal drugs. Antimicrob Agents Chemother 61, e00166–17. [PubMed: 28507115]

Diezmann S, Michaut M, Shapiro RS, Bader GD, and Cowen LE (2012). Mapping the Hsp90 genetic interaction network in *Candida albicans* reveals environmental contingency and rewired circuitry. PLoS Genet 8, e1002562. [PubMed: 22438817]

Donders GGG, Ruban K, Donders F, and Reybrouck R (2022). Lab-based retrospective 10-year analysis shows seasonal variation of vaginal *Candida* infection rates in Belgium. J Clin Med 11, 574. [PubMed: 35160026]

Elbein AD, Pan YT, Pastuszak I, and Carroll D (2003). New insights on trehalose: a multifunctional molecule. Glycobiology 13, 17R–27.

Eleutherio ECA, de Araujo PS, and Panek AD (1993). Role of the trehalose carrier in dehydration resistance of *Saccharomyces cerevisiae*. Biochim Biophys Acta 1156, 263–266. [PubMed: 8461315]

Enjalbert B, Smith DA, Cornell MJ, Alam I, Nicholls S, Brown AJP, and Quinn J (2006). Role of the Hog1 stress-activated protein kinase in the global transcriptional response to stress in the fungal pathogen *Candida albicans*. Mol Biol Cell 17, 1018–1032. [PubMed: 16339080]

Erkut C, Gade VR, Laxman S, and Kurzchalia TV (2016). The glyoxylate shunt is essential for desiccation tolerance in *C. elegans* and budding yeast. eLife 5, e13614. [PubMed: 27090086]

Estruch F (2000). Stress-controlled transcription factors, stress-induced genes and stress tolerance in budding yeast. FEMS Microbiol Rev 24, 469–486. [PubMed: 10978547]

Feofilova EP, Usov AI, Mysyakina IS, and Kochkina GA (2014). Trehalose: chemical structure, biological functions, and practical application. Microbiology 83, 184–194.

Forche A, Abbey D, Pisithkul T, Weinzierl MA, Ringstrom T, Bruck D, Petersen K, and Berman J (2011). Stress alters rates and types of loss of heterozygosity in Candida albicans. mBio 2, e00129–11. [PubMed: 21791579]

Granke LL, and Hausbeck MK (2010). Effects of temperature, humidity, and wounding on development of phytophthora rot of cucumber fruit. Plant Dis 94, 1417–1424. [PubMed: 30743380]

Guan G, Tao L, Yue H, Liang W, Gong J, Bing J, Zheng Q, Veri AO, Fan S, Robbins N, et al. (2019). Environment-induced same-sex mating in the yeast *Candida albicans* through the Hsf1-Hsp90 pathway. PLoS Biol 17, e2006966. [PubMed: 30865631]

Guinea J (2014). Global trends in the distribution of *Candida* species causing candidemia. Clin Microbiol Infect 20, 5–10.

Hassine M, Siah A, Hellin P, Cadalen T, Halama P, Hilbert JL, Hamada W, Baraket M, Yahyaoui A, Legrève A, et al. (2019). Sexual reproduction of *Zymoseptoria tritici* on durum wheat in Tunisia revealed by presence of airborne inoculum, fruiting bodies and high levels of genetic diversity. Fungal Biol 123, 763–772. [PubMed: 31542193]

Hirakawa MP, Chyou DE, Huang D, Slan AR, and Bennett RJ (2017). Parasex generates phenotypic diversity *de novo* and impacts drug resistance and virulence in *Candida albicans*. Genetics 207, 1195–1211. [PubMed: 28912344]

Huang G, Srikantha T, Sahni N, Yi S, and Soll DR (2009). CO_2 regulates white-to-opaque switching in *Candida albicans*. Curr Biol 19, 330–334. [PubMed: 19200725]

Huang G, Wang H, Chou S, Nie X, Chen J, and Liu H (2006). Bistable expression of *WOR1*, a master regulator of white–opaque switching in *Candida albicans*. Proc Natl Acad Sci USA 103, 12813–12818. [PubMed: 16905649]

Jain NK, and Roy I (2009). Effect of trehalose on protein structure. Protein Sci 18, 24–36. [PubMed: 19177348]

Khoo P, Cabrera-Aguas MP, Nguyen V, Lahra MM, and Watson SL (2020). Microbial keratitis in Sydney, Australia: risk factors, patient outcomes, and seasonal variation. Graefes Arch Clin Exp Ophthalmol 258, 1745–1755. [PubMed: 32358645]

Kis-Papo T, Kirzhner V, Wasser SP, and Nevo E (2003). Evolution of genomic diversity and sex at extreme environments: fungal life under hypersaline Dead Sea stress. Proc Natl Acad Sci USA 100, 14970–14975. [PubMed: 14645702]

Li Y, Uddin W, and Kaminski JE (2014). Effects of relative humidity on infection, colonization and conidiation of *Magnaporthe orzyae* on perennial ryegrass. Plant Pathol 63, 590–597.

Lillie SH, and Pringle JR (1980). Reserve carbohydrate metabolism in *Saccharomyces cerevisiae*: responses to nutrient limitation. J Bacteriol 143, 1384–1394. [PubMed: 6997270]

Manstretta V, and Rossi V (2016). Effects of temperature and moisture on development of *Fusarium graminearum* perithecia in maize stalk residues. Appl Environ Microbiol 82, 184–191. [PubMed: 26475114]

Miller MG, and Johnson AD (2002). White-opaque switching in *Candida albicans* is controlled by mating-type locus homeodomain proteins and allows efficient mating. Cell 110, 293–302. [PubMed: 12176317]

Mok WY, Luizão RC, do Socorro Barreto da Silva M, Teixeira MF, and Muniz EG (1984). Ecology of pathogenic yeasts in Amazonian soil. Appl Environ Microbiol 47, 390–394. [PubMed: 6538774]

Ni M, Feretzaki M, Sun S, Wang X, and Heitman J (2011). Sex in fungi. Annu Rev Genet 45, 405–430. [PubMed: 21942368]

Noble SM, and Johnson AD (2005). Strains and strategies for large-scale gene deletion studies of the diploid human fungal pathogen *Candida albicans*. Eukaryot Cell 4, 298–309. [PubMed: 15701792]

Nunn MA, Schäfer SM, Petrou MA, and Brown JRM (2007). Environmental source of *Candida dubliniensis*. Emerg Infect Dis 13, 747–750. [PubMed: 17553256]

O'Brien CE, Oliveira-Pacheco J, Cinnéide EO, Haase MAB, Hittinger CT, Rogers TR, Zaragoza O, Bond U, and Butler G (2021). Population genomics of the pathogenic yeast *Candida tropicalis* identifies hybrid isolates in environmental samples. PLoS Pathog 17, e1009138. [PubMed: 33788904]

O'Meara TR, Veri AO, Polvi EJ, Li X, Valaei SF, Diezmann S, and Cowen LE (2016). Mapping the Hsp90 genetic network reveals ergosterol biosynthesis and phosphatidylinositol-4-kinase signaling as core circuitry governing cellular stress. PLoS Genet 12, e1006142. [PubMed: 27341673]

Opulente DA, Langdon QK, Buh KV, Haase MAB, Sylvester K, Moriarty RV, Jarzyna M, Considine SL, Schneider RM, and Hittinger CT (2019). Pathogenic budding yeasts isolated outside of clinical settings. FEMS Yeast Res 19, foz032. [PubMed: 31076749]

Paul PA, and Munkvold GP (2005). Influence of temperature and relative humidity on sporulation of *Cercospora zeae-maydis* and expansion of gray leaf spot lesions on maize leaves. Plant Dis 89, 624–630. [PubMed: 30795388]

Pfaller MA, Diekema DJ, and International Fungal Surveillance Participant, G. (2004). Twelve years of fluconazole in clinical practice: global trends in species distribution and fluconazole susceptibility of bloodstream isolates of *Candida*. Clin Microbiol Infect 10, 11–23. [PubMed: 14748799]

Reuß O, Vik Å, Kolter R, and Morschhäuser J (2004). The *SAT1* flipper, an optimized tool for gene disruption in *Candida albicans*. Gene 341, 119–127. [PubMed: 15474295]

Rodaki A, Bohovych IM, Enjalbert B, Young T, Odds FC, Gow NA, and Brown AJ (2009). Glucose promotes stress resistance in the fungal pathogen *Candida albicans*. Mol Biol Cell 20, 4845–4855. [PubMed: 19759180]

Schulze U, Larsen ME, and Villadsen J (1995). Determination of intracellular trehalose and glycogen in *Saccharomyces cerevisiae*. Anal Biochem 228, 143–149. [PubMed: 8572270]

Serneels J, Tournu H, and Van Dijck P (2012). Tight control of trehalose content is required for efficient heat-induced cell elongation in *Candida albicans*. J Biol Chem 287, 36873–36882. [PubMed: 22952228]

Sharma B, and Nonzom S (2021). Superficial mycoses, a matter of concern: Global and Indian scenario—an updated analysis. Mycoses 64, 890–908. [PubMed: 33665915]

Singer MA, and Lindquist S (1998). Multiple effects of trehalose on protein folding *in vitro* and *in vivo*. Mol Cell 1, 639–648. [PubMed: 9660948]

Slutsky B, Staebell M, Anderson J, Risen L, Pfaller M, and Soll DR (1987). "White-opaque transition": a second high-frequency switching system in *Candida albicans.* J Bacteriol 169, 189–197. [PubMed: 3539914]

Soveral G, Prista C, Moura TF, and Loureiro-Dias MC (2011). Yeast water channels: an overview of orthodox aquaporins. Biol Cell 103, 35–54.

Sun Y, Gadoury C, Hirakawa MP, Bennett RJ, Harcus D, Marcil A, and Whiteway M (2016). Deletion of a Yci1 domain protein of *Candida albicans* allows homothallic mating in *MTL* heterozygous cells. mBio 7, e00465–00416. [PubMed: 27118591]

Tao L, Cao C, Liang W, Guan G, Zhang Q, Nobile CJ, and Huang G (2014). White cells facilitate opposite- and same-sex mating of opaque cells in *Candida albicans*. PLoS Genet 10, e1004737. [PubMed: 25329547]

Tapia H, Young L, Fox D, Bertozzi CR, and Koshland D (2015). Increasing intracellular trehalose is sufficient to confer desiccation tolerance to *Saccharomyces cerevisiae*. Proc Natl Acad Sci USA 112, 6122–6127. [PubMed: 25918381]

Velásquez AC, Castroverde CDM, and He SY (2018). Plant-pathogen warfare under changing climate conditions. Curr Biol 28, R619–R634. [PubMed: 29787730]

Wallen RM, and Perlin MH (2018). An overview of the function and maintenance of sexual reproduction in dikaryotic fungi. Front Microbiol 9, 503. [PubMed: 29619017]

Wallen RM, Richardson K, Furnish M, Mendoza H, Dentinger A, Khanal S, and Perlin MH (2021). Hungry for sex: differential roles for *Ustilago maydisb* locus components in haploid cells vis à vis nutritional availability. J Fungi 7, 135.

Wiemken A (1990). Trehalose in yeast, stress protectant rather than reserve carbohydrate. Antonie van Leeuwenhoek 58, 209–217. [PubMed: 2256682]

Xiao M, Chen SCA, Kong F, Xu XL, Yan L, Kong HS, Fan X, Hou X, Cheng JW, Zhou ML, et al. (2020). Distribution and antifungal susceptibility of *Candida* species causing candidemia in China: an update from the CHIF-NET study. J Infect Dis 221, S139–S147. [PubMed: 32176789]

Zaragoza O, Blazquez MA, and Gancedo C (1998). Disruption of the *Candida albicans TPS1* gene encoding trehalose-6-phosphate synthase impairs formation of hyphae and decreases infectivity. J Bacteriol 180, 3809–3815. [PubMed: 9683476]

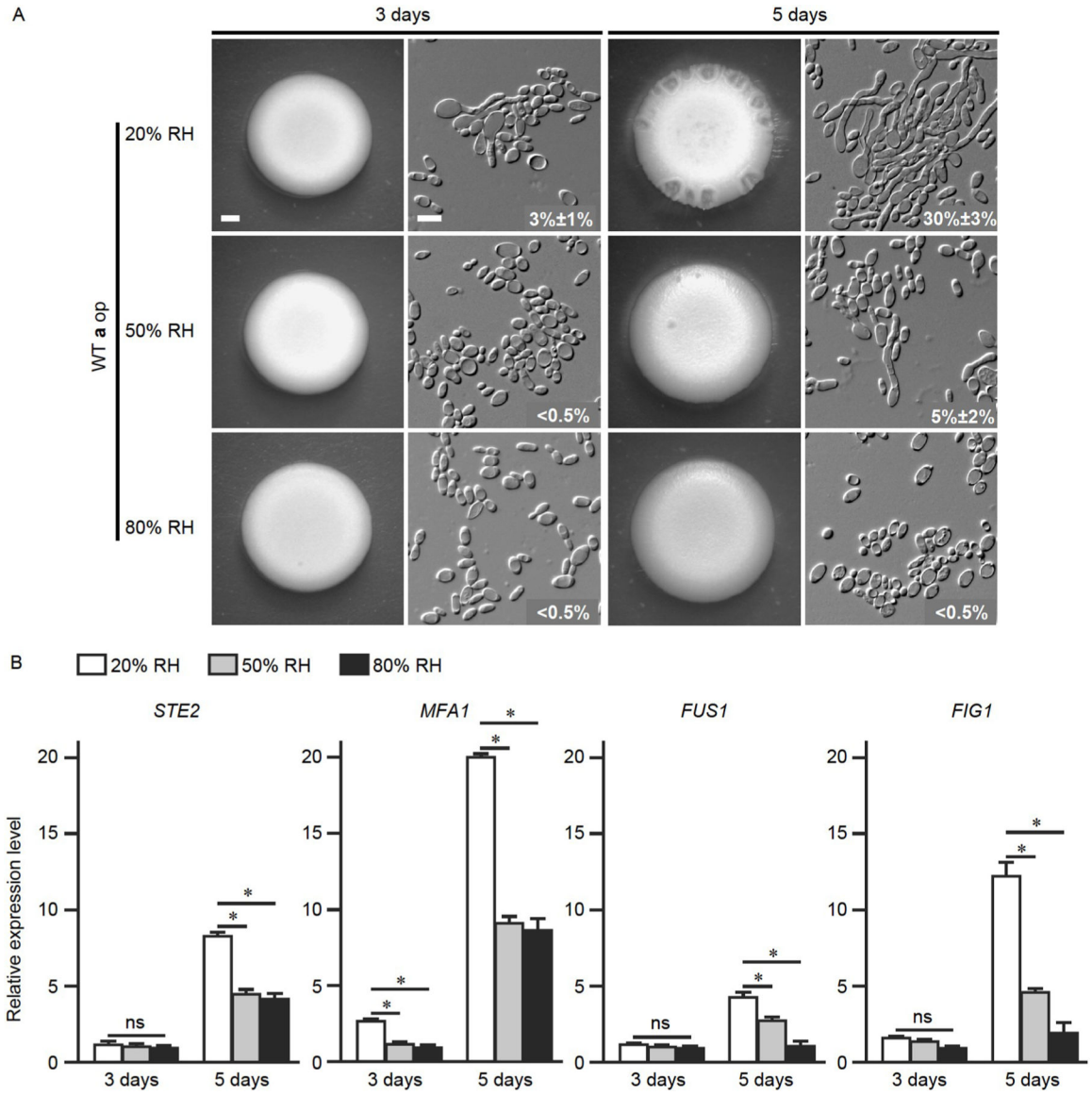

Figure 1.

Development of mating projections by *C. albicans* on YP-K medium plates under different RH conditions. A, Colony and cellular morphologies of the WT strain SN250**a** under 20% RH, 50% RH, and 80% RH conditions. Approximately 1×10^7 opaque cells in 5 μL ddH_2O were spotted onto the YP-K medium and cultured at 25°C for 3 or 5 days under different RH conditions. Percentages of projected opaque cells are indicated in the corresponding cellular morphology images. Data are presented as mean±SD, n=3. Scale bar for colonies, 1 mm; scale bar for cells, 10 μm. B, Relative expression levels of mating-related genes (*STE2*, *MFA1*, *FUS1*, and *FIG1*) under 20% RH, 50% RH, and 80% RH conditions. The strain and culture conditions used were the same as described in panel (A). Error bars represent SD. Three independent experiments were performed. *, P<0.05 (Student's t-tests, two-tailed).

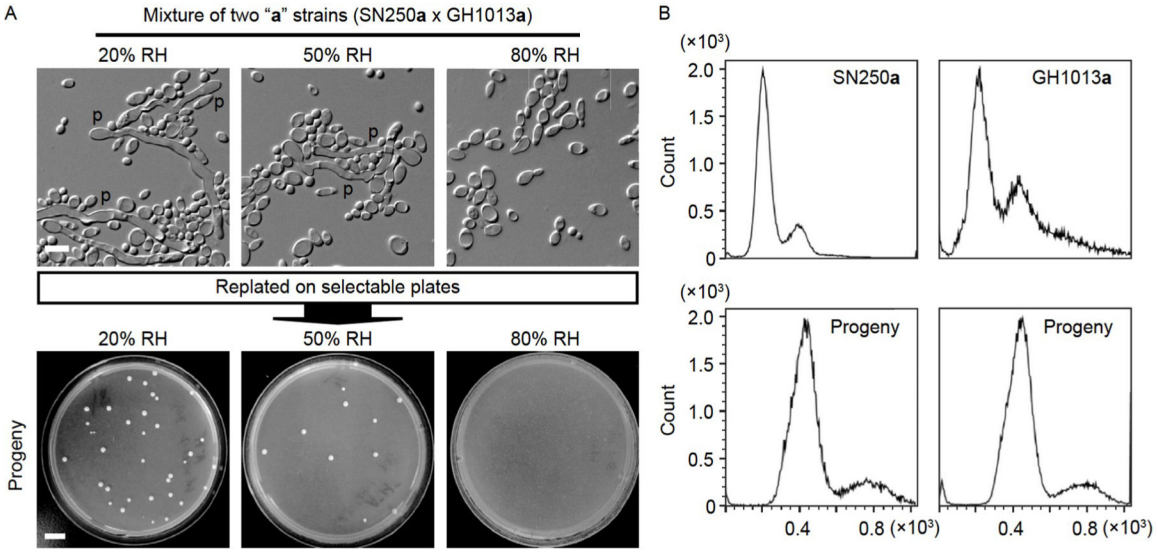

Figure 2.

Low atmospheric humidity promotes same-sex mating in *C. albicans*. A, Same-sex mating between two "**a**" strains. Approximately 1×10^7 opaque cells of each strain (SN250**a** and GH1013**a**) in 10 μL ddH_2O were mixed and spotted onto solid YP-K medium and cultured at 25°C for 5 days under 20% RH, 50% RH, and 80% RH conditions. The mating mixture was collected and replated onto SCD-Arg-His plates for the growth of mating progenies. P, mating projection. Scale bar for plates, 1 cm; Scale bar for cells, 10 μm. B, Flow cytometry analysis of the DNA contents in parental and progeny strains. *C. albicans* cells of single colonies were collected from SCD medium plates and used for flow cytometry analyses.

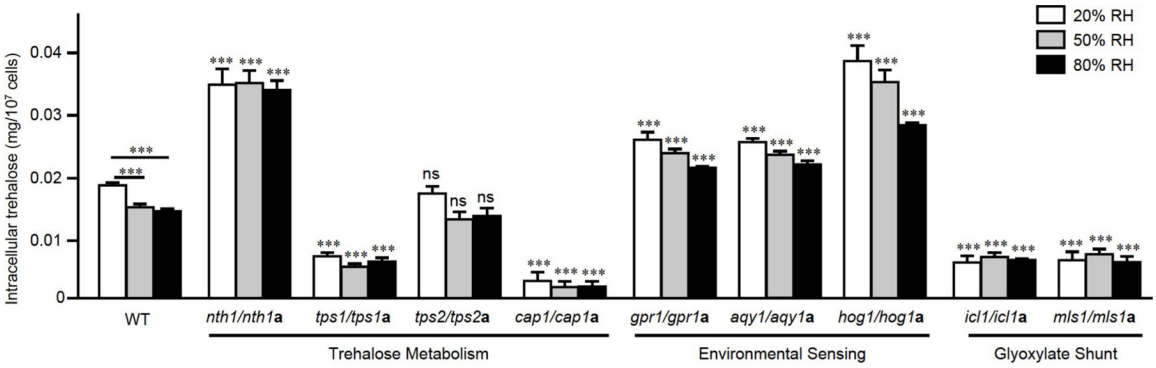

Figure 3.

Low atmospheric humidity promotes trehalose and ROS accumulation in *C. albicans*. Approximately 1×10^7 opaque cells of the WT strain SN250**a**, *nth1*/*nth1***a**, *tps1*/*tps1***a**, *tps2*/*tps2***a**, *gpr1*/*gpr1***a**, *aqy1*/*aqy1***a**, *hog1*/*hog1***a**, *icl1*/*icl1***a**, *mls1*/*mls1***a**, and *cap1*/*cap1***a** mutant strains in 5 μL ddH_2O were spotted onto YP-K medium and cultured at 25°C for 5 days under different RH conditions. 5×10^7 cells were collected for each culture condition and used for intracellular trehalose determination. Error bars represent SD. Three independent experiments were performed. ***, $P<0.0001$ (2-way ANOVA with Tukey's test); ns, no significance.

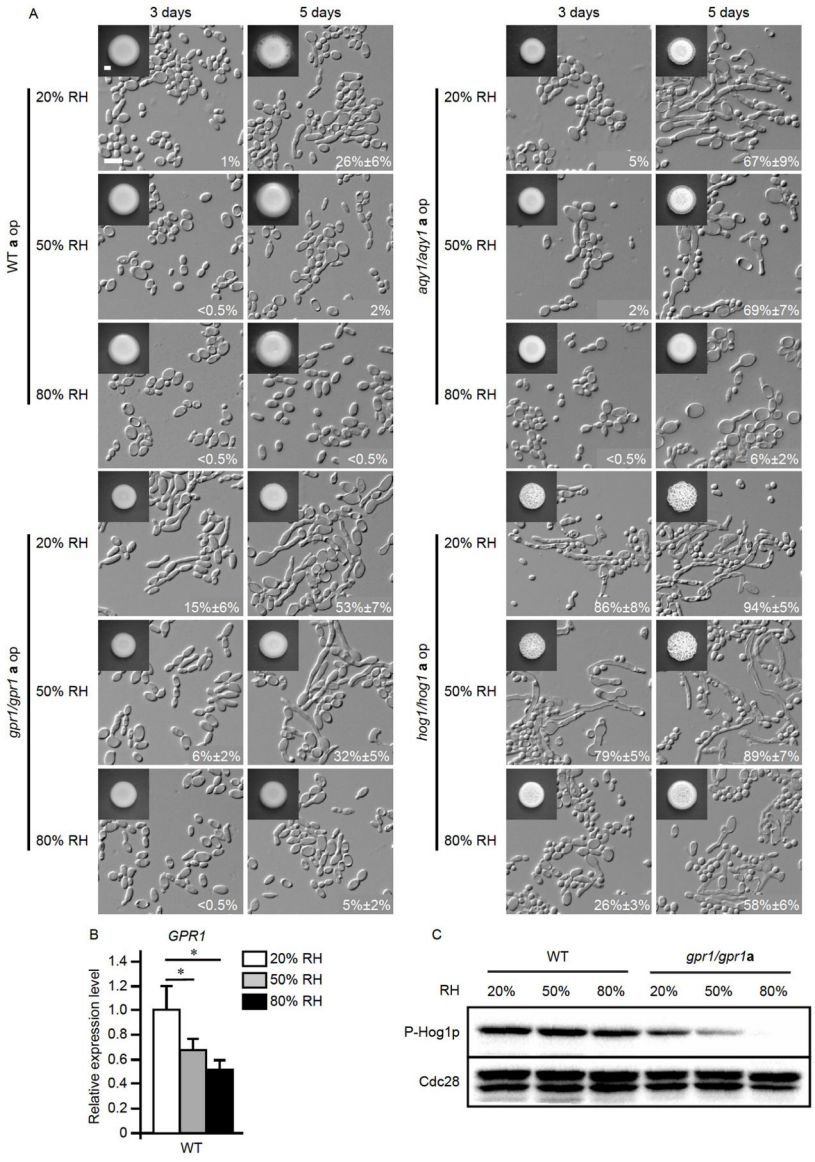

Figure 4.

Gpr1, Aqy1, and Hog1 regulate the development of mating projections in *C. albicans*. A, Colony and cellular morphologies of the WT strain SN250**a**, *aqy1*/*aqy1***a**, *gpr1*/*gpr1***a**, and *hog1*/*hog1***a** mutant strains under different RH conditions. Approximately 1×10^7 opaque cells of the WT strain and mutant strains in 5 μL ddH_2O were spotted onto YP-K medium and cultured at 25°C for 5 days under different RH conditions. Percentages of projected cells are indicated in the corresponding cellular morphology images. Data are presented as mean±SD, n=3. Scale bar for colonies, 1 mm; scale bar for cells, 10 μm. B, Relative expression levels of *GPR1* in the WT strains. Opaque cells (1×10^7) in 5 μL ddH_2O were spotted onto YP-K medium, cultured at 25°C under different RH conditions for 5 days, and then collected for qRT-PCR analyses. WT, SN250**a**. Error bars represent SD. Three independent experiments were performed. *, P<0.05 (Student's t-tests, two-tailed). C, Phosphorylation levels of Hog1 in cells of the WT strain SN250**a** and the *gpr1*/*gpr1***a** mutant

strain. After 5 days of incubation on YP-K medium under different RH conditions, opaque cells were collected for immunoblotting assays. An anti-phospho-p38 antibody (P-Hog1) was used for the determination of Hog1 phosphorylation levels. The levels of Cdc28 protein served as the internal loading control.

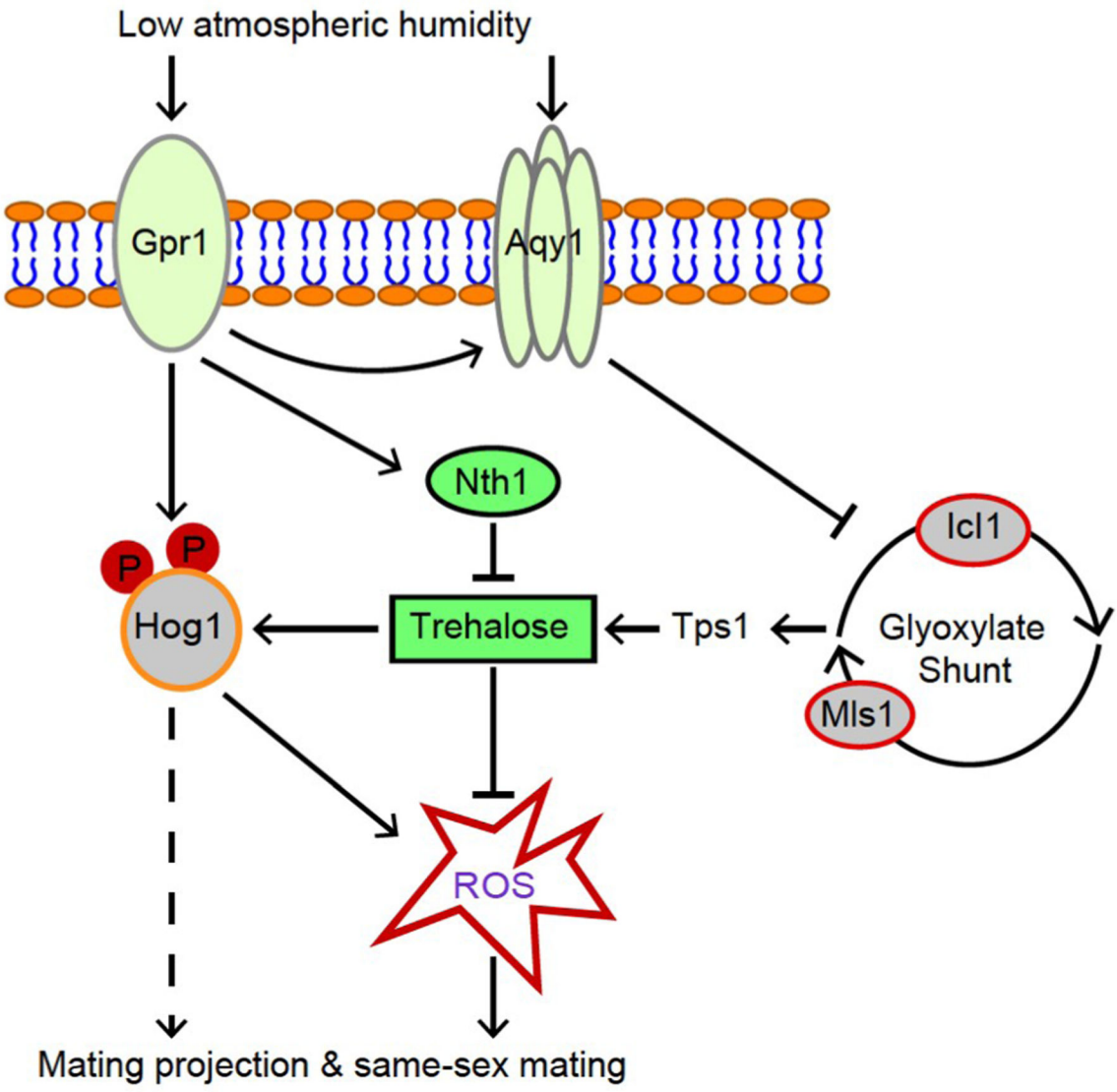

Figure 5.

Regulatory model for low atmospheric humidity-induced mating projection formation and same-sex mating in *C. albicans*. Cell membrane proteins Gpr1 and Aqy1 serve as surface sensors of atmospheric humidity. Intracellular trehalose and ROS function as central regulators of low atmospheric humidity-induced mating projection formation and same-sex mating. Low atmospheric humidity induces the increase of both trehalose and ROS levels in *C. albicans*, which coordinate to synergistically promote mating. Increased levels of trehalose lead to osmotic stress. The ROS and osmotic stresses induce the development of mating projections and same-sex mating. Trehalose has a protective effect against intracellular stress. Inactivation of the trehalose synthases Tps1, Icl1, or Mls1, which are required for efficient production of trehalose, leads to an increase in intracellular oxidative stress.

Table 1

Same-sex mating efficiencies of the WT and mutant "**a**" cell crosses of *C. albicans* under different RH conditions[a)]

No.	Cross	Mating efficiency		
		20% RH (fold change compared with 80% RH[*])	50% RH (fold change compared with 80% RH[*])	80% RH (fold change compared with the WT cross[**])
1	WT**a**1×WT**a**2	$(1.1\pm0.2)\times10^{-6}$ (>37-fold)	$(1.2\pm0.4)\times10^{-7}$ (>4-fold)	$<2.9\times10^{-8}$
2	*nth1*/*nth1***a**×*nth1*/*nth1***a**	$(1.4\pm0.1)\times10^{-5}$ (1.4-fold)	$(1.2\pm0.2)\times10^{-5}$ (1.2-fold)	$(1\pm0.3)\times10^{-5}$ (>345-fold)
3	*gpr1*/*gpr1***a**×*gpr1*/*gpr1***a**	$(1.1\pm0.1)\times10^{-5}$ (13-fold)	$(1\pm0.1)\times10^{-5}$ (12-fold)	$(8.2\pm1.7)\times10^{-7}$ (>28-fold)
4	*hog1*/*hog1***a**×*hog1*/*hog1***a**	$(1.4\pm0.2)\times10^{-5}$ (1.6-fold)	$(8.9\pm1.1)\times10^{-6}$ (1-fold)	$(8.6\pm1.9)\times10^{-6}$ (>297-fold)
5	*tps1*/*tps1***a**×*tps1*/*tps1***a**	$(1.1\pm0.2)\times10^{-5}$ (3-fold)	$(7.9\pm0.6)\times10^{-6}$ (2-fold)	$(3.3\pm0.9)\times10^{-6}$ (>114-fold)
6	*icl1*/*icl1***a**×*icl1*/*icl1***a**	$(1.4\pm0.2)\times10^{-5}$ (5-fold)	$(6.7\pm0.7)\times10^{-6}$ (2-fold)	$(2.8\pm0.4)\times10^{-6}$ (>97-fold)
7	*mls1*/*mls1***a**×*mls1*/*mls1***a**	$(1.4\pm0.2)\times10^{-5}$ (6-fold)	$(5.6\pm0.7)\times10^{-6}$ (2-fold)	$(2.3\pm0.6)\times10^{-6}$ (>79-fold)
8	*aqy1*/*aqy1***a**×*aqy1*/*aqy1***a**	$(8.0\pm0.8)\times10^{-6}$ (9-fold)	$(2.1\pm0.3)\times10^{-6}$ (2-fold)	$(8.7\pm0.3)\times10^{-7}$ (>30-fold)
9	*cap1*/*cap1***a**×*cap1*/*cap1***a**	$(7.2\pm0.8)\times10^{-8}$ (>3-fold)	$<1.9\times10^{-8}$ (NA)	$<2.3\times10^{-8}$ (NA)

[a)] WT**a**1, SN250**a** (*arg4Δ*/*Δ*); WT**a**2, GH1013**a** (*ura3Δ*/*Δ*). The two mating partners of each mutant strain were arginine-auxotrophic (*arg4Δ*/*Δ*) and histidine-auxotrophic and (*his1Δ*/*Δ*). The quantitative mating assays were performed at 25°C for 5 days under the conditions of 20% RH, 50% RH, and 80% RH. **a**, *MTL***a**/*Δ*; *MTL* locus, mating type like locus.

[*], The fold changes of mating efficiencies under 20% RH and 50% RH compared with that of the same mating cross under 80% RH.

[**], The fold changes of mating efficiencies of the mutant strains compared with that of the WT strain mating cross No. 1 (WT**a**1×WT**a**2) under 80% RH.

Table 2

Proportion of mating projection of the WT and mutant "**a**" cells under the different RH conditions[a)]

WT and mutants		Proportion of mating projection		
		20% RH (%)	50% RH (%)	80% RH (%)
WT (SN250**a**)	3 days	4±2	<0.5	<0.5
	5 days	28±5	9±3	<0.5
nth1/*nth1***a**	3 days	17±5	<0.5	<0.5
	5 days	47±6	45±7	8±3
pbs2/*pbs2***a**	3 days	23±3	25±4	16±2
	5 days	71±6	73±4	43±4
tps1/*tps1***a**	3 days	19±5	17±4	22±4
	5 days	78±8	75±6	68±5
tps2/*tps2***a**	3 days	8±3	5±3	<0.5
	5 days	38±3	10±4	<0.5
icl1/*icl1***a**	3 days	43±4	54±6	<0.5
	5 days	88±5	85±8	25±2
mls1/*mls1***a**	3 days	44±4	48±3	<0.5
	5 days	86±6	85±7	22±3
cap1/*cap1***a**	3 days	<0.5	<0.5	<0.5
	5 days	5±2	<0.5	<0.5
tetON-HSF1/*hsf1*	3 days	44±3	51±5	71±7
	5 days	85±3	82±4	86±5
tetON-HSF1/*hsf1*+50 μg mL^{-1} Dox	3 days	53±3	57±5	77±3
	5 days	91±5	90±4	92±3
tetON-HSP90/*hsp90*	3 days	21±3	22±4	24±2
	5 days	45±6	43±7	36±4
tetON-HSP90/*hsp90*+50 μg mL^{-1} Dox	3 days	34±3	32±4	34±6
	5 days	85±5	82±6	87±3
cwt1/*cwt1***a**	3 days	47±4	45±5	21±5
	5 days	80±3	77±6	45±4
cwt1/*cwt1***a**	3 days	<0.5	<0.5	<0.5

WT and mutants		Proportion of mating projection		
		20% RH (%)	50% RH (%)	80% RH (%)
nth1/*nth1-NTH1p-NTH1*	5 days	<0.5	<0.5	<0.5
	3 days	2	<0.5	<0.5
	5 days	27±5	2	<0.5
aqy1/*aqy1-AQY1p-AQY1*	3 days	<0.5	<0.5	<0.5
	5 days	35±5	5	<0.5
gpr1/*gpr1-GPR1p-GPR1*	3 days	<0.5	<0.5	<0.5
	5 days	24±2	4	<0.5
hog1/*hog1-HOG1p-HOG1*	3 days	5	<0.5	<0.5
	5 days	34±5	8±2	<0.5
tps1/*tps1-TPS1p-TPS1*	3 days	1	<0.5	<0.5
	5 days	28±5	3	<0.5

*a)*The mating projection assays were performed after the culture at 25°C for 3 or 5 days under the conditions of 20% RH, 50% RH, and 80% RH. To calculate the proportion of mating projection, the number of projected opaque cells in 3 independent views (a total of 300 opaque cells were present) was counted. Data are presented as mean±SD. **a**, *MTL***a**/*Δ*; *MTL* locus, mating type like locus; Dox, doxycycline.